Journal of Hydrology: Regional Studies 50 (2023) 101579

Contents lists available at ScienceDirect

Journal of Hydrology: Regional Studies

journal homepage: www.elsevier.com/locate/ejrh

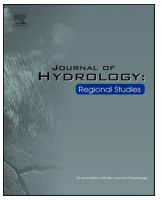

Unraveling hydroclimatic forces controlling the runoff coefficient trends in central Italy's Upper Tiber Basin

Arash Rahi [a,c,*], Mehdi Rahmati [b,c], Jacopo Dari [a,d], Carla Saltalippi [a], Cosimo Brogi [c], Renato Morbidelli [a]

[a] Dept. of Civil and Environmental Engineering, University of Perugia, via G. Duranti 93, 06125 Perugia, Italy
[b] Department of Soil Science and Engineering, Faculty of Agriculture, University of Maragheh, Maragheh, Iran
[c] Institute of Bio and Geosciences (IBG), Forschungszentrum Jülich, 52428 Jülich, Germany
[d] National Research Council, Research Institute for Geo-Hydrological Protection, via Madonna Alta 126, 06128 Perugia, Italy

ARTICLE INFO

Keywords:
Runoff coefficient
Soil Water Storage
LULC changes
Wavelet Coherency Analysis
Mann-Kendall test

ABSTRACT

Study region: This study refers to the Upper Tiber basin at the Ponte Nuovo outlet in central Italy.
Study focus: This study aims at analyzing runoff coefficient (Rc) trends and connections with hydroclimatic parameters, namely (temperature (T), precipitation (P), soil water storage (SWS), and LULC (Land Use Land Cover) changes) using Mann-Kendall (MK) test and wavelet coherence analysis (WCA).
New hydrological insights for the region: The results show a decreasing Rc over 1927–2020, coupled with increasing T and decreasing SWS based on seasonal MK test, and implications for water resource management in Central Italy. Results underscore the need for sustainable hydrological management paradigms to address challenges posed by scarcity of water resources under unpredictable changing climate. Rc-hydroclimatic parameters correlations through WCA revealed complex hydrological interactions. Precipitation exhibited insignificant and erratic patterns from 1950 to 1978, and while it established more significant correlations with Rc from 1990 to 2020, it remained moderately erratic. Conversely, weak correlation found against LULC changes, concurrently with strong positive but lagged correlation with SWS (1 month), and strong lagged (3–6 months) but negative correlation with T indicate the prevailing significance of hydroclimatic factors over LULC changes. These insights underscore the pivotal role of hydroclimatic factors in shaping regional water resources. Policymakers can harness these insights as a bedrock to develop effective strategies for water resources planning and climate change adaptation.

1. Introduction

Climate change has affected different aspects of hydrological cycle on a global scale (IPCC, 2022). The anticipated impacts of global climate change on water resources and the environment, both globally and locally, are expected to be significant and threatening. Climate change drives changes in the water cycle, amplifying droughts, floods, glacier melt, sea-level rise, and storms (Sivakumar, 2011), and is widely recognized as a significant factor contributing to the reduction in water resource availability and altering their spatial distribution on a global scale (Kundzewicz et al., 2008). Impact of climate change is apparent in various regions worldwide such

* Corresponding author at: Dept. of Civil and Environmental Engineering, University of Perugia, via G. Duranti 93, 06125 Perugia, Italy.
E-mail address: arash.rahi@studenti.unipg.it (A. Rahi).

https://doi.org/10.1016/j.ejrh.2023.101579
Received 9 August 2023; Received in revised form 5 October 2023; Accepted 15 November 2023

as Europe (Bauwens et al., 2011; Bosshard et al., 2014; Baattrup-Pedersen et al., 2018; Fonseca and Santos, 2019), Asia (Yang et al., 2014; Dey and Mishra, 2017; Khanal et al., 2021), Africa (Arnell, 1999; Descroix et al., 2009; Ndhlovu and Woyessa, 2021), and America (Rouse et al., 1997; Sperna Weiland et al., 2012). Compared to continental regions, the Mediterranean has a more intensive flash flood regime which might be attributed to the strong impact of antecedent saturation levels on runoff coefficient (Marchi et al., 2010). In Italy, this topic has been a subject of much scrutiny, as reported by Maragno et al. (2018), Darvini and Memmola (2020), and Piro et al. (2018). The runoff coefficient (Rc), defined as the ratio between the runoff and rainfall amounts (Bedient et al., 2008; Burak et al., 2021), was first conceptualized during the early twentieth century (Sherman, 1932), and is still widely used in the engineering practices (Rose and Peters, 2001; Ha et al., 2019; Chen et al., 2020). In hydrologic designs Rc frequently represents as a key input parameter and diagnostic variable to reflect runoff generation in a catchment (Merz et al., 2006). It is also useful to understand runoff dynamics and available streamflow as it can be used as an index of the catchment response to rainfall (Zhang et al., 2014).

Climate variability indirectly affects flood mechanisms by altering rainfall seasonality, impacting watershed moisture conditions for each storm event (Sivapalan et al., 2005). In fact, precipitation and discharge have a significant relationship in terms of basin's annual water balance (Ceballos and Schnabel, 1998). Rainfall depth and soil water content are known to be key factors influencing surface runoff (Rascón-Ramos et al., 2021). According to Penna et al. (2011), the mean value of Rc increases with mean annual P, and the spatial distribution of Rc is closely connected with this parameter. Above all, meteorological changes, including increased annual temperatures, sunshine hours, and wind speeds, significantly enhance evapotranspiration, contributing to the declining trends in runoff and Rc, as highlighted by Shao et al. (2010). It is reported that annual Rc is inversely correlated with annual mean T and directly correlated with annual P (Chen et al., 2007).

Rainfall and temperature can impact Rc by influencing soil moisture, as key influencer of Rc variation (Penna et al., 2011; Zehe et al., 2010), although, the relationship between Rc and antecedent soil moisture was observed to be insignificant in some cases (Li et al., 2016). Norbiato et al. (2009) reported a significant linear relationship between Rc and Mean Annual Precipitation (MAP), which may influence Rc distribution by governing initial conditions, like soil moisture variability. Bertola et al. (2021) found that flood changes in southern Europe are influenced by both antecedent soil moisture and intensive rainfall. Initial soil moisture is positively correlated with Rc (Liu et al., 2020) and it highly controls the Rc variation at both basin (Merz and Blöschl, 2009) and plot (Song and Wang, 2019) scales.

Human activities have impacted land use and land cover (LULC) during the past few decades (Guo et al., 2021; Regasa et al., 2021). Changes in LULC modify the energy and water fluxes between the atmosphere and the Earth's surface and have an impact on the climate system's dynamics (Chahine, 1992; Boulain et al., 2009). LULC changes, particularly alterations in agricultural areas, forested areas, and urbanization, have a significant linear correlation with runoff generation, as reported by Astuti et al. (2019). Among different LULC changes, transition of forest and grasslands into farmed and urbanized areas can have several effects on river flows (Birhanu et al., 2019). Total discharge and peak flows increase as forested areas decline because of agricultural activities and urbanization (Truong et al., 2018; Robinet et al., 2018). As an example, widespread deforestation in Slovakia caused the rising of estimated design floods (Danáčová et al., 2020). Forest cover positively influences the Rc for multiple return periods, while agricultural land expansion and deforestation reduce the Rc during peak floods (Sriwongsitanon and Taesombat, 2011).

Within this framework, it is essential to assess Rc changes in river basins due to climatic and human-induced factors (Velpuri and Senay, 2013). A decreasing trend of observed runoff in sub-Saharan Africa, southern Europe, southernmost South America, southern Australia, and western mid-latitude North America was reported by Milly et al. (2005). Trend analysis is an effective method to detect changes in climatic and hydrological components (Asfaw et al., 2018; Tan et al., 2019). The Mann-Kendall (MK) test has been widely used to detect trends in reference evapotranspiration, streamflow, T, and P time series in different regions worldwide (Yue and Wang, 2004; Xu et al., 2010; Asfaw et al., 2018; Morbidelli et al., 2018; Gedefaw et al., 2019; Tadese et al., 2019; Dari et al., 2023). However, we believe that combination of MK test with wavelet coherence analysis (WCA) (Si, 2008) can provide more insight about the time-frequency relationship of the detected trends. Grossman and Morlet (1984) introduced the wavelet transform analysis to the field of Earth sciences, which has become increasingly popular in several geoscience sectors to assess the strength and latency of a correlation in nonstationary data sets in time and frequency domains (Graf et al., 2014). In his review, Labat (2005) suggested new wavelet-based tools to hydrologists to improve wavelet analysis. Subsequently, the wavelet transform technique has found applications in various fields. For example, Vargas et al. (2010) utilized wavelet transform to assess field-scale time series of soil CO_2 production. Lauzon et al. (2004) applied this technique in catchment studies of soil moisture, while Labat et al. (2004) used it to investigate the temporal variability of Amazon basin hydrology. Furthermore, Rahmati et al. (2020) utilized the wavelet transformation to evaluate the coherence and phase shift between soil water content and evapotranspiration.

While Rc and its controlling factors have been extensively studied, our research stands out by applying MK analysis to examine Rc trends and potential control factors using long-term in situ data in the Mediterranean conditions of central Italy. Furthermore, we employed WCA to investigate simultaneous and lagged correlations between Rc and these control factors in both time and frequency domains. This approach innovatively enables us to explore the evolution of the relationship between Rc and studied control factors over time and detect possible changes in their relationships, particularly in response to extreme events such as droughts, extreme precipitation, and land use changes.

2. Materials and methods

2.1. Study area

The Tiber River basin is located in the central part of Italy. Its water catchment is the largest in the central Apennines and covers an

area of almost 17500 km^2 which includes 6 administrative regions and 12 provinces. Almost 90% of this area is located in the Umbria and Lazio regions, while the remaining 10% falls within the regions of Emilia-Romagna, Tuscany, Marche and Abruzzo. Aside from Rome, the major cities that are located within the basin include Perugia, Terni, and Rieti. The Tiber River originates at an altitude of 1268 m asl on the slopes of Monte Fumaiolo (1407 m asl) in Emilia-Romagna and flows 405 km from there southwards in the south part of Rome and finally into the Tyrrhenian Sea. The basin also includes several lakes, among them Trasimeno Lake (122.7 km^2), Piediluco Lake (1.7 km^2), Vico Lake (12.3 km^2) and Albano Lake (6.0 km^2). The Tiber basin is predominantly mountainous throughout the northern and eastern parts and is characterized by the presence of sub-flat surfaces and by a predominance of slopes between 20% and 40%. An overview of the study area, which comprises the Upper Tiber basin at Ponte Nuovo outlet (in Umbria region) and extends over 4147 km^2 with an average altitude of 523 m asl, is given in Fig. 1. The study area comprises 36 meteorological stations distributed all around the basin (meteorological stations in Fig. 1a). The study area is characterized by a Mediterranean climate, with hot summers and rainfall events, prevalent from autumn to spring, characterized by frontal processes coming from the Tyrrhenian Sea. The natural covered area represents around 72% of the basin and is the biggest land use area. It is followed by agricultural areas (26%) and urban areas, which represent just around 2% of covered area.

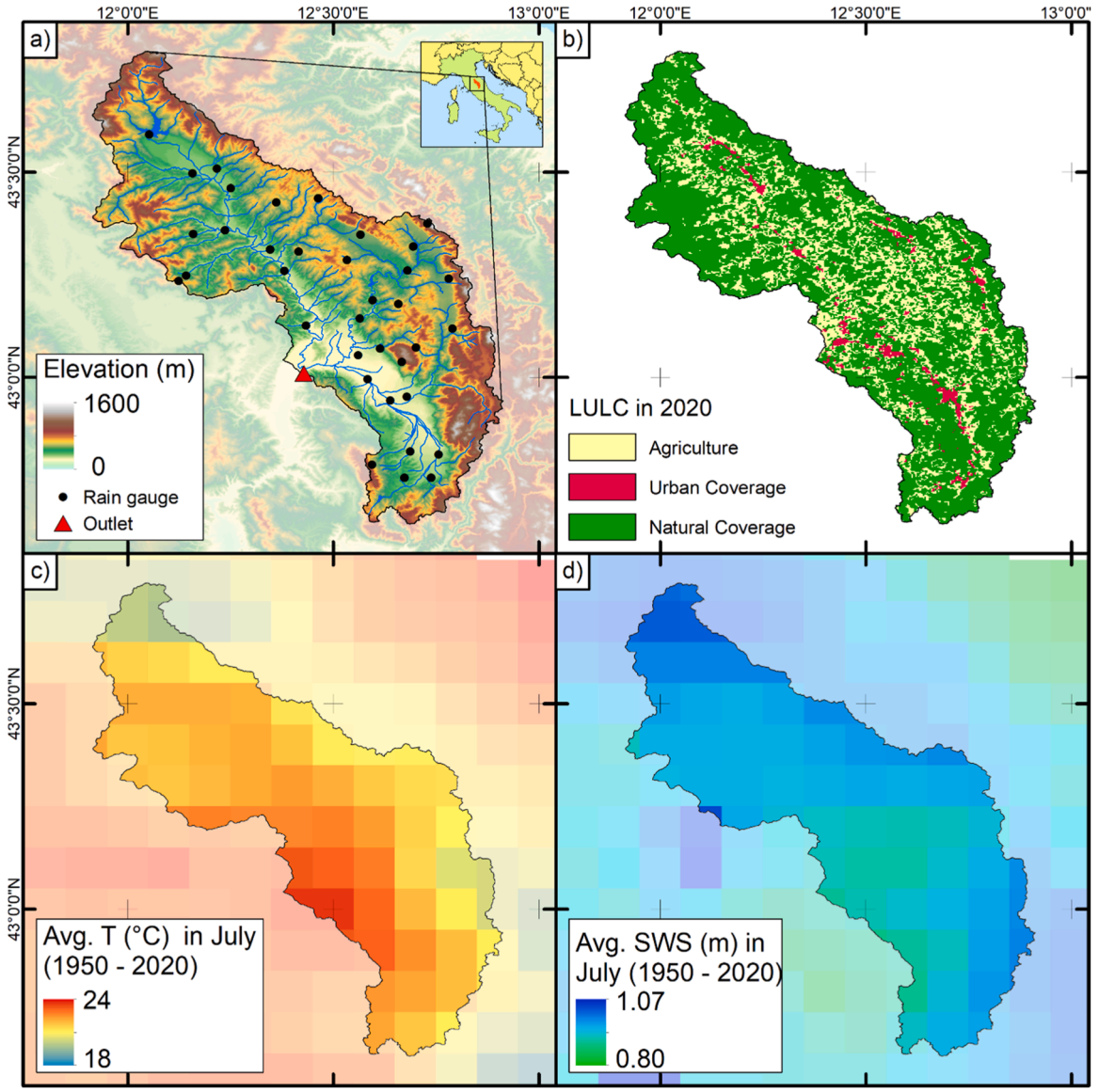

Fig. 1. Overview of the study area: (a) digital elevation map of the Upper Tiber basin at Ponte Nuovo outlet (b) land use land cover, LULC, map in 2020 (c) average monthly temperature, T, (°c) in July from 1950 to 2020 (d) average monthly soil water storage, SWS, (m) in July from 1950 to 2020.

2.2. Hydroclimatic parameters

In the present study, Rc represents the ratio between the height of outflow (runoff) and P calculated at the monthly time scale. Monthly-cumulated outflow volumes observed at the closing section of Ponte Nuovo outlet is available in digital format by the Servizio Idrografico Regione Umbria (SIR-RU, https://servizioidrografico.regione.umbria.it/). The height of outflow, then, has been calculated by dividing the volume by the area of the basin. Concerning P, the data has been obtained from 36 meteorological stations within the study area. In particular, for the period 1927–1993, the historical data of the rainfall depths has been collected from the hydrological annals provided by the Istituto Superiore la Protezione e la Ricerca Ambientale (ISPRA, https://www.isprambiente.gov.it/). From 1994–2020, the P data is made available by SIR-RU. The cumulative monthly values measured by each rain gauge have been collected for all considered years, and the Thiessen polygons method was used to obtain the basin-averaged monthly P data.

The average monthly data of T from 1950 to 2020 was obtained from Copernicus ERA5-Land (European Reanalysis v5- Land) service (Muñoz-Sabater et al., 2021) with a 9 km spatial sampling.

The average monthly data of volumetric soil water content (SWC) from 1950 to 2020 were also obtained from the Copernicus ERA5-Land data set. To quantify the SWS, the first 4 layers of the product's physical schematization were considered (up to a depth of 2.89 m).

Due to the presence of an 11-year data gap from 1979 to 1989, the observation time series was divided into 2 sub-periods a) from 1927 to 1978 (52 years) and b) from 1990 to 2020 (31 years). The WCA was then performed separately in each period.

2.3. LULC changes

LULC information was obtained from the Climate Change Initiative (CCI) of the European Space Agency (ESA). The data covers the period from 1992 to 2020 with a spatial resolution of 300 m. The 22 land cover classes of the data set were grouped into 3 main categories, namely agricultural coverage, urban coverage, and natural coverage (see Table 1). Time series of the differences in each category percentage with respect to its temporal mean (i.e., mean-centered differences) were analyzed.

2.4. Data assessment

Table 2 shows the data sources used in this study. Records pertaining to runoff and Rc were not available between 1979 and 1989, corresponding to a missing data rate of 11.7% over the study area. To ensure consistency across the temporal range of the timeseries, adjustments were necessary as it is necessary to use continuous timeseries while implementing WCA between Rc and monthly parameters. In addition, SWS and T time series begin in 1950. These issues were solved by dividing the dataset into two distinct time spans (i.e., 1950–1978 and 1990–2020) as this was the only suitable solution. The data used in this study had different resolutions. However, the focus of our study was to examine the Rc and its possible trends. Since the Rc represents an integrated effect of losses in the watershed and is a watershed-level variable, all other variables are also brought to the watershed level by aggregating or averaging the data from all pixels and points within the study area. Based on Table 2, WCA between Rc and LULC changes was performed with yearly temporal resolution.

Fig. 2 illustrates the yearly time series of Rc in the study area from 1927 to 2020 together with the linear trend line. A slight decreasing trend on Rc is observable by trend line inspection. Although observed trend can be considered as a notable indicator to comprehend the hydrology of given basin, a more effective means of managing catchment conditions and accounting for seasonal effects is to conduct trend analyses on yearly and seasonal parameters using the MK test and implementing WCA techniques through the Upper Tiber basin at Ponte Nuovo outlet.

2.5. MK trend analysis

In this study, seasonal time series of Rc, P, runoff, T and SWS were calculated for the study area. To compute seasonal time series, data was divided into four seasons of winter (January to March), spring (April to June), summer (July to September) and autumn (October to December). Trend analyses of the seasonal time series were determined using the MK test as nonparametric method at the confidence levels of 95% or ($p < 0.05$).

The Mann-Kendall test (Mann, 1945; Kendall, 1975) is based on correlation between rank and correlation of time series. For a given time series $\{X_i, i = 1, 2\ldots, n\}$, the null hypothesis H0 (no trend or trend-free) assumes it is independently distributed, and the

Table 1
Land cover categories and subcategories based on global classes of the CCI-LC maps.

Agricultural coverage	Urban coverage	Natural coverage
Cropland rainfed Cropland irrigated or post flooding Mosaic cropland	Bare area Urban area	Mosaic natural vegetation, Tree covers broadleaved* , Tree cover needle leaved* , Tree cover mixed leaf type, Shrublands, Mosaic tree and shrub, Mosaic herbaceous cover, Grassland, Lichens and mosses, Sparse vegetation, Tree cover flooded* , Shrubs or herbaceous cover flooded

*For these classes, all sub-classes were included

Table 2
Applied databases description.

Data	Temporal resolution	Spatial resolution	Data source
P	Monthly, 1927–2020	In situ	ISPRA_SIR-RU
Runoff	Monthly, 1927–2020 (exclude 1979–1989)	In situ	ISPRA_SIR-RU
SWC	Monthly, 1950–2022	9 km (~0.08°)	ERA5-land services
T	Monthly, 1950–2022	9 km (~0.08°)	ERA5-land services
LULC	Annual, 1992–2020	300 m	CCI_C3S

DEM: digital elevation map; SWC: soil water content; CCI: climate change initiative; C3S: Copernicus climate Change service

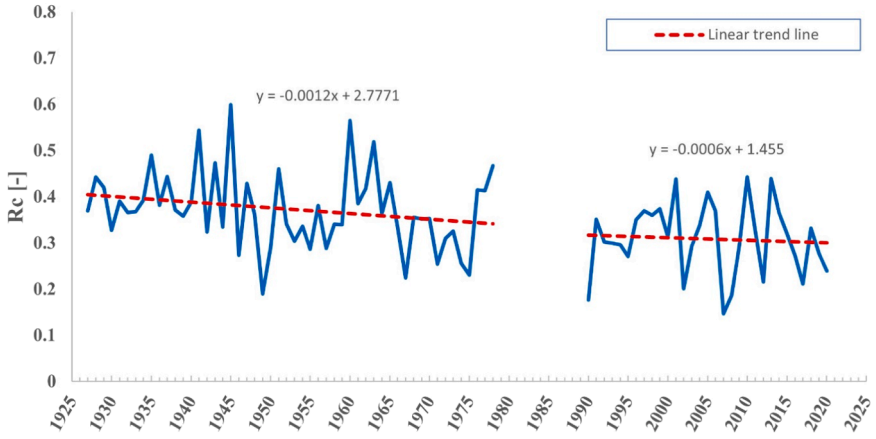

Fig. 2. . Time series of annual Rc in the Upper Tiber at Ponte Nuovo outlet from 1927 to 2020, 5-year moving average trendline is shown by dashed line.

alternative hypothesis H1 (existing trend) is that a monotonic trend exists.

The standardized test statistic (Z) of the MK test is respectively given by:

$$Z = \begin{cases} \dfrac{S-1}{\sqrt{VAR(S)}} S > 0 \\ 0 \text{if } S = 0 \\ \dfrac{S+1}{\sqrt{VAR(S)}} \text{if } S < 0 \end{cases} \quad (1)$$

The standardized MK statistic Z follows the standard normal distribution (Mean (Z) = 0 and Var (Z) = 1), and the null hypothesis is rejected if the absolute value of Z is larger than the theoretical value $Z_{1-\alpha/2}$ (for two-tailed test) or $Z_{1-\alpha}$ (for one-tailed test), where α is the statistical significance level. $Z_{1-\alpha/2}$ is the $1-\alpha/2$ quantile of the standard normal distribution. In this study, α is set to be 0.05. Therefore, a positive or negative Z values indicate an upward or downward trend, respectively. At the significance level of 0.05, if $p \leq 0.05$ corresponding to $|Z| > 1.96$, then the existing trend is statistically significant.

2.6. Wavelet coherence analysis

To determine distribution of the correlation between two signals, the continuous WCA was applied between Rc and other examined variables (i.e., P, SWS, T and LULC changes). Grinsted et al. (2004) introduced the MATLAB (MathWorks Inc., Natick, Massachusetts) software package of WCA to check the relationships in time frequency spaces between two time series using the Monte Carlo method to assess the significance of coherence. The integral wavelet transform, $W(s,\tau)$, of a time series $y(t)$observed at time t is defined by Si (2008) as follows:

$$W(s,\tau) = \int y(t).\frac{1}{\sqrt{s}}\Psi^*\left(\frac{t-\tau}{s}\right)dt \quad (2)$$

where ψ* indicate the mother wavelet function, s is the contraction ($s < 1$) or dilation ($s > 1$) or factor of the wavelet function ψ*, and τ is the temporal shift of the mother wavelet function (Si, 2008).

The normalized part of the cross-wavelet spectrum, also called coherence coefficient (CC), can be compared with R^2 (coefficient of determination) value in conventional correlation analysis. In contrast to R^2 values obtained from conventional correlation analysis, CC is localized both in the time and frequency domains, however, it is restricted to the linear part of that relation. After removing any

potential phase shift (or delay, which is the difference in timing of two consecutive maximal values of investigated signals), it shows the maximum correlation between two signals (Graf et al., 2014). With the use of wavelet cross-correlation, it is possible to efficiently determine the degree of correlation and delay between two processes at a given scale (Labat, 2005). In the present study the phase shift has been evaluated between Rc (benchmark signal) and P, SWS, T and LULC changes time series. The following equation is used to quantify the phase shift between a base signal (Rc) and a second signal (e.g., SWS) (Rahmati et al., 2020):

$$\text{Phase shift} = \frac{\text{Phase angle}}{2\pi} \times m \tag{3}$$

where m stands for the period (1/frequency) of the signals, and phase shift (in month) and phase angle (in radians) refer to the difference in timing of two following maximal values of the base and second signals, such as the maximal of Rc and SWS. By using cross wavelet spectra and wavelet coherence analysis, the phase angle is quantified. Hence, we analyze the coherence of the second signal (examined hydrological variables) in accordance with the first signal (Rc). Here, the phase angles have been changed from radians to phase shifts in months to provide a simpler interpretation of the results.

3. Results

The findings of this study are presented in two distinct sections. The first one comprises the MK test outcomes of seasonal parameters summarized in Table 2. These were evaluated during specified time intervals. The subsequent section pertains to the WCA and encompasses the time frames spanning from 1950 to 1978 and 1990–2020.

3.1. Trend analysis

Table 3 presents the results referring to MK test applied to Rc, P, Runoff, SWS, and T. MK analysis of P shows significant decreasing trend from 1927 to 2020 for all seasons except of summer when no significant trend is observed. Autumn, winter, and spring exhibit higher negative slopes respectively, indicating a more pronounced decline in P during these seasons. Similarly, a significant decreasing trend during all seasons is found for runoff from 1927 to 2020. The analysis of the runoff trend slope shows that it decreases the most in winter and the least in summer. MK test of Rc does not show a significant trend from 1927 to 2020 for any season except summer when a significant decreasing trend is detectable. Although the analysis of Rc did not reveal a statistically significant trend in winter, spring, and autumn, a negative slight slope can be observed. An indication of a significant downward trend of SWS is pointed out by MK test at 95% of confidence level from 1950 to 2020 during winter, spring, and summer. The analysis shows no significant trend for autumn although a slight decrease with refer to trend slope value is found. Also, a slight decreasing slope is observable in winter, spring, and

Table 3
Seasonal trends of the investigated hydroclimatic parameters in the Upper Tiber at Ponte Nuovo outlet according to the MK test during (a) 1927–2020 or (b) 1950–2020.

Components	Winter	Spring	Summer	Autumn
	Trend Slope P-value Z	Trend Slope P-value Z	Trend Slope P-value Z	Trend Slope P-value Z
P[a]	Decreasing -0.070 0.033* -2.13	Decreasing -0.054 0.037* -2.07	No trend 0.026 0.345 0.942	Decreasing -0.102 0.018* -2.35
Runoff[a]	Decreasing -0.070 0.001* -3.226	Decreasing -0.036 0.001* -3.305	Decreasing -0.006 0.001* -3.123	Decreasing -0.038 0.002* -3.019
Rc[a]	No trend -0.0002 0.252 -1.144	No trend -0.0002 0.130 -1.512	Decreasing -0.001 0.020* -2.317	No trend -0.0001 0.396 -0.843
SWS[b]	Decreasing -0.00014 0.033* -2.12	Decreasing -0.00017 0.013* -2.47	Decreasing -0.00015 0.008* -2.63	No trend -0.00008 0.345 -0.94
T[b]	Increasing 0.006 0.026* 2.21	Increasing 0.008 0.039* 2.06	Increasing 0.007 0.018* 2.35	No trend 0.005 0.190 1.30

(*) confidence level of 95%
P-value stand for probability value
Z stand for standardized MK statistic

summer, while it reduced to half of magnitude during autumn. The trend analysis of T shows a significant increasing trend for all the seasons except autumn during the 1950–2020 period. In this case, the increasing trend for autumn is detectable albeit insignificantly. The ratio of increasing slope in all seasons is almost equal with highest slope in spring. The investigation of LULC changes by using MK in the Upper Tiber at Ponte Nuovo outlet shows that natural LULC (Nat LULC) changes (rate of modifying natural coverage to other land covers) were significantly decreasing from 1992 to 2020. There was no significant trend for agricultural LULC (Agr LULC) changes during this period; however, the positive slope shows an insignificant upward trend. Based on Table 4, MK test reveals a significant trend for urban LULC (Ur LULC) changes that indicate urbanization was increasing from 1992 to 2020 at the 95% of confidence level. Evaluating the slope values of these land covers showed a slight positive change of AgrLULC, while substantial negative and positive changes in NatLULC and Ur LULC occurred respectively.

3.2. WCA between Rc and key parameters

The WCA has been carried out to analyze the key hydrological and meteorological parameters that may affect the runoff generation in the studied area. Our findings were satisfactory, as they unveiled main hydroclimatic factors controlling Rc over study area. T was found to be the most influential one, and SWS exhibited rapid effectiveness in runoff generation with minimal phase shift. Future research should explore previously unconsidered variables like evapotranspiration and groundwater and their interactions with Rc in the study area. As described in section 2.4, hydroclimatic timeseries are divided in two distinct periods (i.e., 1950–1978 and 1990–2020). Various scenarios may arise during the wavelet analysis of the base and second signals. For a more comprehensive understanding of these possible scenarios, refer to Fig. A in Appendix A, which serves as an informative guide for an improved interpretation of our methodology.

3.2.1. WCA between Rc and P

The results show that over the study area from 1950 to 1978 the coherence between Rc and P is unstable and fluctuating. However, a weak trend at different periods of 8–16 months (centered at yearly cycle) is apparent in Fig. 3a. The coherence analysis from 1990 to 2020 reveals a strong relation between Rc and P in yearly cycle. As correlation is almost continuous during this cycle, coherence in other periods such as monthly and seasonal cycles is unsteady. The almost right-aligned direction of the arrows in Fig. 3b indicates a positive correlation between Rc and P. Above all, the visual comparison between the panel (a) and (b) reveals that Rc at yearly circle is more coherent with P in the second period (1990–2020) compared to the first one (1950–1978) for the investigated catchment.

Fig. 3c-d show that CC at yearly cycle is highly fluctuating in both periods 1950–1978 and 1990–2020. As Fig. 3c shows, the period of 1956–1962 has an acceptable coherency in the pilot basin starting from 0.7 and reaching the maximum value of 0.85 at the beginning of 1960. In the remaining years, Rc was less correlated to P. Fig. 3d shows that, in the annual cycle, coherence oscillates between 0.5 and 0.8 from 1990 to 2020 and correlation between Rc and P becomes more stable over the last 3 decades.

The direction of arrows in panels (a) and (b) indicates several variations with time, although correlation remains generally positive from 2004 onwards. Inspection of the arrow direction in the yearly cycle of Fig. 3a shows nearly identical upward arrows, revealing that the examined variables lagged behind each other with a negative phase shift value.

The average phase shift between Rc and P is quantified for the annual cycle in Fig. 3e-f. Panel (e) of Fig. 3 shows a negative phase shift between Rc and P in the period of 1956–1961. This indicates a phase shift value of less than 3 months between Rc and P, and simply means that Rc is lagging behind P (i.e., the maximum of P occurs around 3 months earlier than the maximum of Rc). Fig. 3f shows that the phase shift between Rc and P during 1990–2020 lasts less than 4 months meaning that any increase in P results in an increase in Rc but with a lag value of less than 4 months. Referring to Fig. 3b, changing arrow directions before 2004 and consistent upward and right alignment afterwards, indicating positive correlation between Rc and P with a phase shift of less than 3 months (a quarter of yearly cycle). This pattern reminds of how during the past decade a positive correlation is stabilized between Rc and P in a yearly cycle in the study area.

3.2.2. WCA between Rc and average SWS

The relationship between Rc and basin-averaged SWS for different times and frequencies has been investigated by using WCA. The results show that in the study area, from 1950 to 1978, there is a strong coherence between Rc and SWS in the yearly cycle, especially from 1956 to 1969 (see Fig. 4a). The coherence analysis from 1990 to 2020 (Fig. 4b) shows a strong correlation between Rc and SWS at yearly cycle from 1997 to 2014, while the coherence in other cycles including monthly and seasonal cycles is unsteady and erratic. The direction of arrows (mostly right aligned) indicates a positive correlation between these variables. Fig. 4c illustrates that CC generally

Table 4
Trends of the annual LULC changes in the Upper Tiber at Ponte Nuovo outlet according to the MK test during 1992–2020.

Components	Temporal resolution	Trend	Slope	P-value	Z
Agr LULC changes	Annual	No Trend	0.006	0.764	0.300
Nat LULC changes	Annual	Decreasing	-0.038	4e-10*	-6.248
Ur LULC changes	Annual	Increasing	0.035	5e-14*	7.528

(*) confidence level of 95%
P-value stand for probability value
Z stand for standardized MK statistic

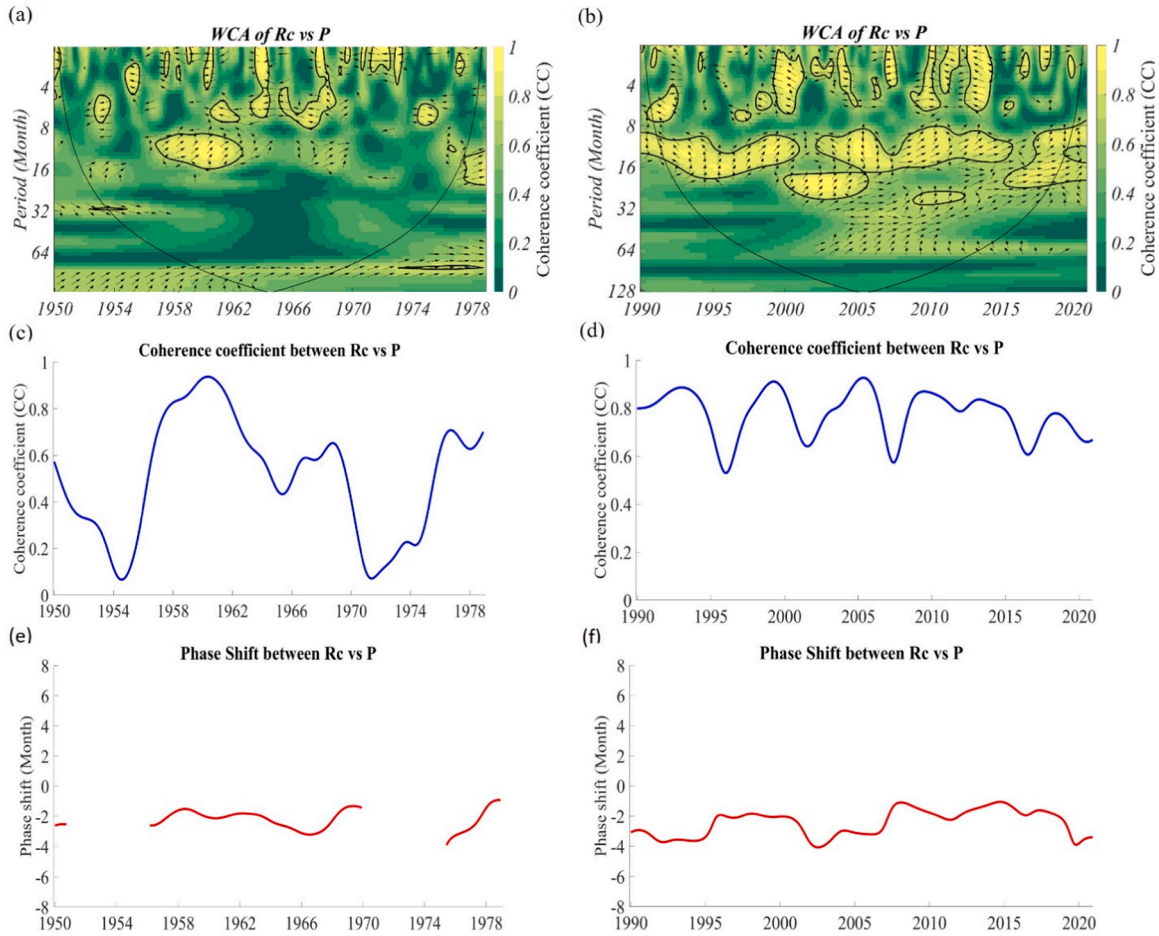

Fig. 3. WCA between Rc and P in the Upper Tiber at Ponte Nuovo outlet during (a)1950–1978 and (b)1990–2020, the 95% significance level is shown as a thick contour. CC between Rc and P during the period of yearly cycle (c)1950–1978 and (d)1990–2020; phase shift between Rc and P during the period of yearly cycle (e)1950–1978 and (f)1990–2020. Panel (e) does not include the section where the CC < 0.5 (insignificant).

varies between 0.3 and 0.9, with the highest values (0.7–0.9) occurring during 1956–1969. Referring to Fig. 4d, CC has a high range of variation from 0.1 to 0.9 but it stays strong from 1997 to 2014 with a range of 0.7–0.9.

The right-aligned horizontal arrows in Fig. 4a, indicating a positive correlation between Rc and SWS during the annual cycle without any phase shift or with a shift whose magnitude is lower than a quarter of yearly cycle. As illustrated in Fig. 4e, a phase shift of less than a month occurs from 1957 to 1969. Fig. 4f shows no phase shift between Rc and SWS from 1998 to 2014. The sudden alteration in Fig. 4f is apparent due to the modification of the direction of arrows, either from upward right-aligned to downward right-aligned, or vice versa, because of a change in the leading variable. As the coherence during the occurrence of these discontinuities was insignificant (CC < 0.5), further speculation on this is avoided. It is noteworthy that another question raises from this issue: why did the coherence between the studied signals become insignificant during these periods, while it is significant before and after? We have tried to answer this question, but could not find a reasonable explanation, thus concluding that further investigation must be done by considering more signals (variables). It seems that an unknown event, which is not captured in our considered time series, decorrelates the studied signals in these periods.

3.2.3. WCA between Rc and T

The wavelet analysis between Rc and T shows a substantial correlation between the two variables in the pilot basin in a yearly cycle. Regarding the other cycles (monthly or seasonal), an inconsistent and localized coherence occurs in the pilot basin (Fig. 5). Fig. 5a indicates that Rc is highly correlated with T from 1957 to 1970 and the identical left-aligned arrows direction showed anti-correlation between Rc and T over the study area. Moreover, Fig. 5b shows strong coherency between Rc and T from 1998 to 2017 at the yearly cycle, while the horizontal left-aligned arrows show anti-correlation between the above-mentioned parameters in the Upper Tiber at Ponte Nuovo outlet.

Fig. 5c demonstrates the CC between Rc and T over pilot basin and it is apparent that, from 1958 to 1969, a robust correlation is taking place (values between 0.7 and 0.85). Fig. 5d exhibits the high coherence between Rc and T at the period of 12 months. Here, the

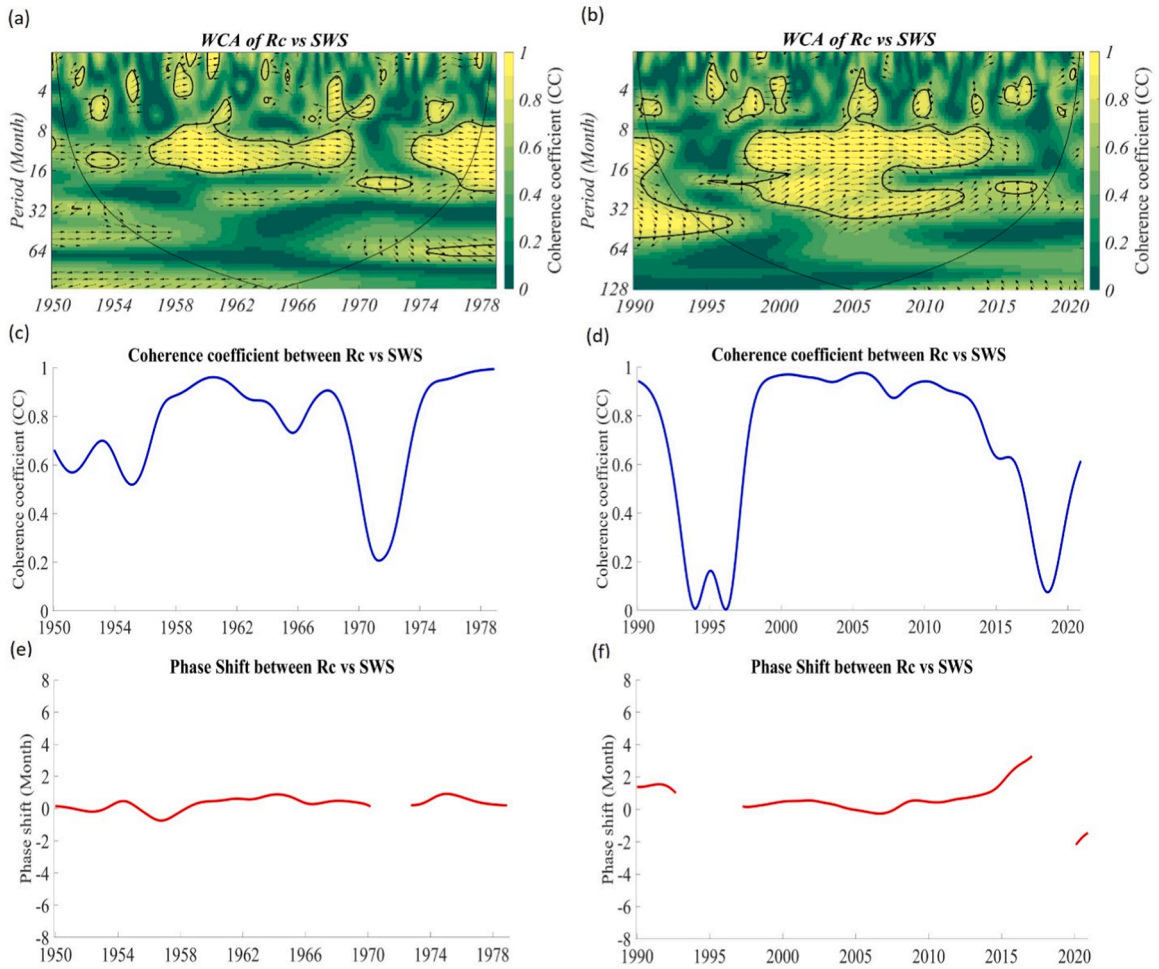

Fig. 4. WCA between Rc and average SWS in the Upper Tiber at Ponte Nuovo outlet during (a)1950–1978 and (b)1990–2020, the 95% significance level is shown as a thick contour. CC between Rc and SWS during the period of yearly cycle (c)1950–1978 and (d)1990–2020; phase shift between Rc and SWS during the period of yearly cycle (e) 1950–1978 and (f) 1990–2020. Panel (e) and (f) do not include the section where the CC < 0.5 (insignificant).

coherence fluctuates between 0.7 and 0.9 from 1998 to 2013. It started from 0.9 and, after a decreasing trend for 15 years, it reached 0.7 in 2013.

As shown in Fig. 5, the highest CC can be observed at yearly cycle. Fig. 5a shows a strong anti-correlation from 1958 to 1970. Moreover, the left-aligned and almost downward arrows show a phase shift ranging between a quarter and a half of cycle, which is equal to a phase shift of 3–6 months between Rc and T (Fig. 5e). Moreover, the downward direction of arrows indicates positive phase shifts; hence, T is controlling Rc.

In Fig. 5b the same trend of Fig. 5a can be observed from 1998 to 2014, therefore, as shown in Fig. 5f, there was a phase shift of 3–6 months between Rc and T. Above all, from 1998 to 2014, the nearly downward direction of arrows indicating positive phase shift which particularly means that T is controlling the Rc.

3.2.4. WCA between RC and LULC changes

The analysis of the coherence between Rc and LULC changes in the Upper Tiber at Ponte Nuovo outlet is shown in Fig. 6. A weak correlation is apparent between Rc and LULC changes referring to the considered categories. Fig. 6a shows that, in the period of 2 years during the interval 1996–2003, there is a weak correlation between Rc and Agr LULC changes. Also, the left aligned arrows show a negative correlation. Fig. 6b shows that, in the period of 2 years, there is a correlation between Rc and Nat LULC changes. The generally left aligned arrows at 2011–2018 shows the negative correlation. Fig. 6c illustrates no correlation between Rc and Ur LULC changes. Fig. 6d shows a CC that ranges between 0 and 0.55 in the examined area, starting from 0.1 in 1992 and increasing to 0.55 in 2000 before decreasing again. In Fig. 6e, CC ranges between 0 and 0.8. It started from 0.1 in 1992 and rose to 0.8 in 2015. The CC between 2010 and 2019 is significant. Low CC between Rc and Ur LULC is shown in Fig. 6f, which ranges between 0 and 0.4 (not significant).

Fig. 6g shows that the phase shift between Rc and Agr LULC changes varies by less than 1 year, and according to the generally

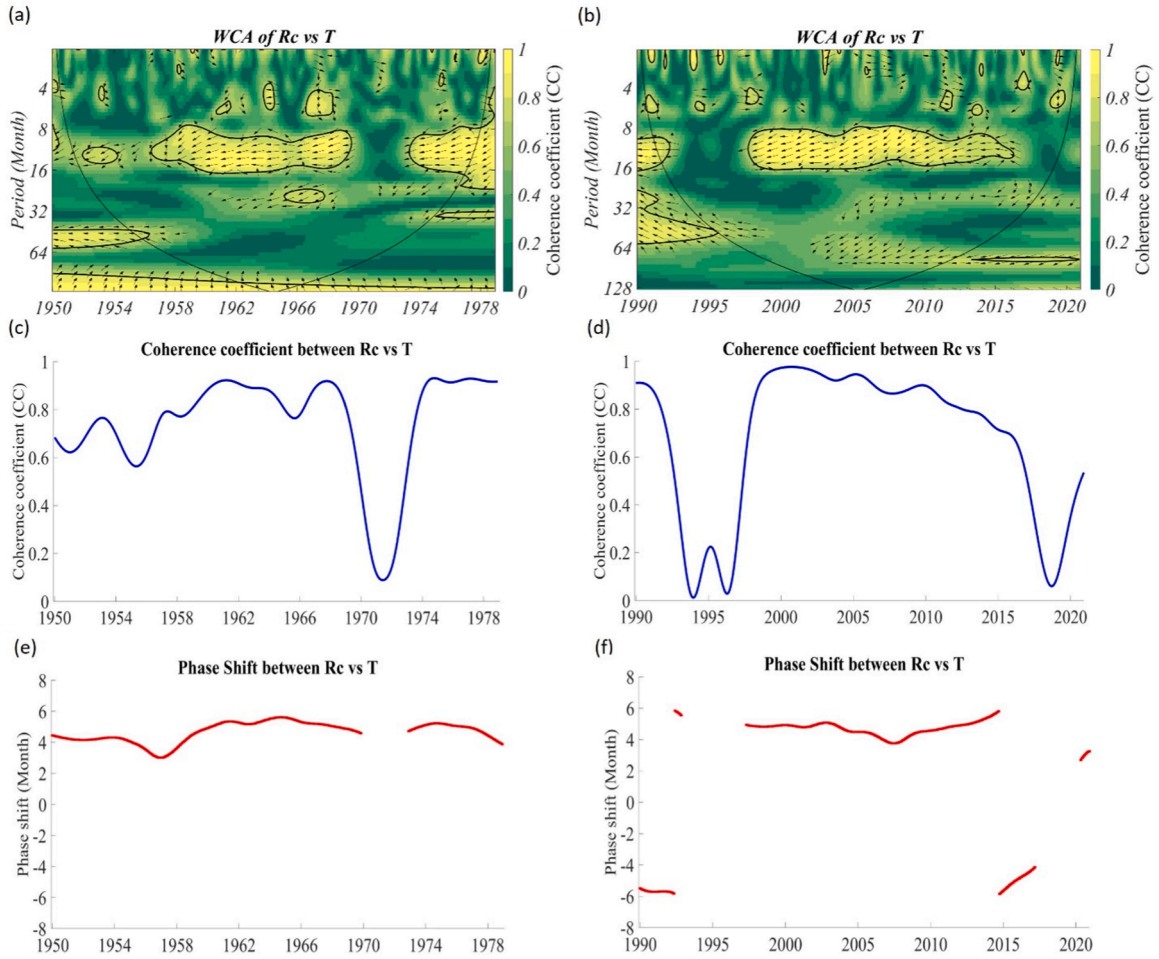

Fig. 5. WCA between Rc and average T in the Upper Tiber at Ponte Nuovo outlet (a)1950–1978 and (b)1990–2020, the 95% significance level is shown as a thick contour. CC between Rc and T during the period of yearly cycle (c)1950–1978 and (d)1990–2020; phase shift between Rc and T in the Upper Tiber at Ponte Nuovo outlet during the period of yearly cycle (e)1950–1978 and (f)1990–2020. Panel (e) and (f) do not include the section where the CC < 0.5 (insignificant).

upward arrows, it is negative. Fig. 6h illustrates an anti-correlation between Rc and Nat LULC changes at the period of biennial cycle from 2010 to 2019 and, according to the direction of arrows, in the period of 2010–2018 the phase shift value is positive. Fig. 6i shows that phase shift value between Rc and Ur LULC changes are changing several times, hence, it is not reliable.

4. Discussion

Europe's temperature has raised doubling the global average in the past 30 years, at + 0.5 °C per decade from 1991 to 2021 (WMO, 2022). Consistent with WMO report, trend analysis of T shows a significant increasing trend in most seasons from 1950 to 2020 in the study area (Table 3). Due to energy-limited nature, precipitation is anticipated to rise globally at a rate of 2–3% per degree of warming (Schneider et al., 2017). The consensus is that precipitation patterns vary temporally and spatially; however, an increase in global mean precipitation and short-term extremes is expected, both increasing and decreasing trends are anticipated at continental and regional scales (Dore, 2005). Uncommonly, the Mediterranean region may see increased extreme precipitation along with reduced total rainfall (Alpert et al., 2002). The findings of this study, which are consistent with earlier ones focused on the Mediterranean basin (Longobardi and Villani, 2010; Altava-Ortiz et al., 2011; Gentilucci et al., 2019), indicate that the long-term seasonal P is on the decline during all seasons except of summer (non-significant increasing, see Table 3). MK test of runoff showed that statistically decreasing trends are prominent for all seasons in the study area from 1927 to 2020. A similar decreasing trend is reported in southern Europe (Milly et al., 2005) and in five different catchments in Italy (Darvini and Memmola, 2020). An analysis of 433 major global river basins (1985–2014) showed a predominant Rc decrease in northern Europe, Eastern Asia, and northeast America with minor increase in regions like central and South Africa, Australia, and North America (Xiong et al., 2022). Precipitation is the factor that impacts the most to runoff due to climate change (Li et al., 2022). Therefore, significant decreasing trends of P (except for summer) and runoff

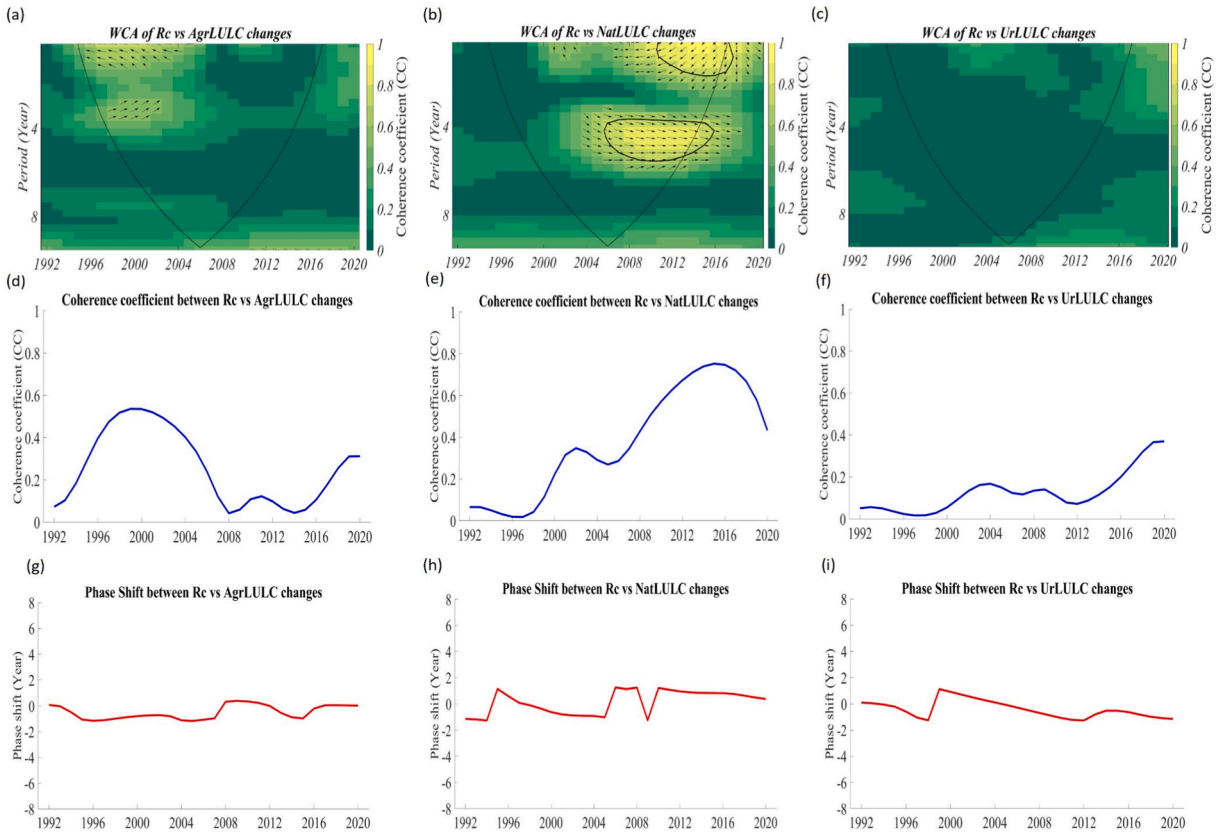

Fig. 6. WCA between Rc and LULC changes in the Upper Tiber at Ponte Nuovo outlet (a) Agr LULC, (b) Nat LULC and (c) Ur LULC, the 95% significance level is shown as a thick contour. CC between Rc and LULC changes during the period of 2-year (d) Agr LULC, (e) Nat LULC and (f) Ur LULC; phase shift between Rc and LULC changes in the Upper Tiber at Ponte Nuovo outlet during the period of biennial cycle (g) Agr LULC, (h) Nat LULC and (i) Ur LULC.

during 1927–2020 validate this correlation. MK test for SWS revealed a significant winter, spring, and summer downward trend from 1950 to 2020. For example, summer soil moisture exhibits a consistent drying trend in Europe (Qiao et al., 2021) and in central Europe (Zawadzki et al., 2014). Penna et al. (2011) introduced soil moisture content as a key influencer of Rc variation. The decreasing trend of SWS from 1950 to 2020 may associate with less surface runoff and, therefore, a decreasing trend of Rc. Sheffield and Wood (2008) reported a switch to a drying trend in subsequent years, coinciding with rising temperatures locally and globally. Although precipitation variations drive droughts, temperature's influence has intensified in the past decade.

Our findings are aligned with the pertinent decreasing trend in northern Europe and globally, but there is still lack of research on controlling Rc distribution and key factors influencing basin responses to climate changes in the Mediterranean and at regional scales. As the main objective, WCA quantified correlation and phase shift between Rc and key variables, the results highlighted this method as straightforward and well-established for producing reliable insights to the complexity of hydrological cycle. WCA indicates a fluctuating Rc- P correlation across times and frequencies, hindering a clear relationship. However, the phase shift between Rc and P peaked at approximately 4 months in 2002–2003, then decreased towards 1 month by 2015. This suggests increased Rc sensitivity to P after the severe drought in western and central Europe in 2003. Here, from February 2003 to June 2004, the amount of precipitation was below average (Rebetez et al., 2006). Monthly average temperatures exceeded long-term averages by over 4 °C, coinciding with a shortage of precipitation, especially during the summer of 2003.

Global warming and the consequent increase in T in Europe played a central role in the hydrology of the Upper Tiber basin at Ponte Nuovo basin. Based on the results, Rc and T had a substantial negative correlation in yearly cycle with a 3–6-month phase shift. During 1957–1970 and 1998–2014, T played a key role in controlling Rc and affecting all parameters, including the runoff generation system. The consequence of temperature peaks lasting for a phase shift period was highlighted. Based on wavelet analysis, Rc had high positive correlation with the SWS and the near-zero phase shift underscores the importance of SWS in investigating catchment characteristic and water management. WCA between Rc and Agr LULC changes showed a weak correlation, Rc and Nat LULC changes represented stronger correlation. Finally, there was no correlation between Rc and Ur LULC. As Wilk and Hughes (2002) noted, the complexity of a large river basin can conceal the impact of LULC change on hydrological responses. Moreover, LULC changes covering only 1.8% of the total study area might not be significant enough to create a distinct change in the water yield.

In summary, our innovative regional approach employed MK tests and WCA, revealing a general Rc decrease and addressing water

resource management challenges while enhancing hydrological understanding and identifying controlling factors and correlations. T emerged as the most influential hydrometeorological factor, with parameters like SWS showing less phase shift and effectiveness in flash flood management. Although LULC changes had minimal impact in the pilot basin, their influence may be greater in larger, more anthropized catchments. This approach addresses common water challenges in the Mediterranean area, emphasizing variables with reduced phase shift for Rc peak forecasting and improved hydrological model calibration. Further investigation, using higher temporal resolution wavelet analysis at a larger scale, could enhance our understanding of key influencer parameters in the runoff generation system.

5. Conclusions

This study examined Rc trend over the Upper Tiber basin at Ponte Nuovo outlet catchment over a period of almost a century and unravelled the hydroclimatic factors mostly controlling it. The main findings can be listed as follows:

1. Rc during 1927–2020 reveals a decreasing trend for all the seasons although significant in summer only.
2. Seasonal P and runoff observations from 1927 to 2020 exhibited significant decreases in all seasons except for P in summer. SWS showed a significant decreasing trend from 1950 to 2020 in all seasons except for autumn. MK test of seasonal T shows a significant increasing trend for all the seasons from 1950 to 2020 except for winter.
3. There is a strong positive correlation between Rc and SWS at both investigated periods (1950–1978 and 1990–2020) during the yearly cycle with a phase shift of less than 1 month between these two variables. A substantial negative correlation between Rc and T at both investigated periods in yearly circle is observable, highlighting a phase shift of 3–6 months. From 1950–1978, the correlation between Rc and P showed instability and fluctuations but became strongly associated on an annual cycle from 1990 to 2020. WCA between Rc and LULC changes showed a weak correlation between agricultural and natural changes and Rc whereas no correlation was found for Ur LULC changes.

Based on the results found, Rc is more affected by hydrological and climatic variables than LULC changes in the investigated area. WCA highlighted T as proactive key parameters as it can control the Rc, while SWS recognized as a key parameter can affect the Rc with less phase shift in a faster interaction. The results have significant implications for water resources management in central Italy, emphasizing the need for sustainable hydrological management to tackle water resources decline with an unfolding climate.

CRediT authorship contribution statement

Arash Rahi: Conceptualization, Formal analysis, Investigation, Methodology, Software, Validation, Visualization, Writing – original draft, Writing – review & editing. **Mehdi Rahmati:** Conceptualization, Investigation, Methodology, Resources, Supervision, Validation, Visualization, Writing – review & editing. **Jacopo Dari:** Conceptualization, Investigation, Methodology, Resources, Supervision, Validation, Visualization, Writing – review & editing. **Carla Saltalippi:** Investigation, Resources, Writing – review & editing. **Cosimo Brogi:** Visualization, Writing – review & editing. **Renato Morbidelli:** Conceptualization, Investigation, Methodology, Resources, Supervision, Validation, Visualization, Writing – review & editing.

Declaration of Competing Interest

The authors declare that they have no known competing financial interests or personal relationships that could have appeared to influence the work reported in this paper.

Data availability

Data will be made available on request.

Acknowledgements

The authors wish to thank Elena Santucci for the technical support. The authors acknowledge the Hydrographic Service of the Umbria region for proving part of the data used in this study.

Appendix A. defining parameters of wavelet coherency analysis

The correlation between two time series and an estimation of the phase shift between them can be obtained by using WCA. Basic concepts such as positive correlation, anti-correlation, phase shift, phase angle, period, frequency, and direction of arrows have been described to facilitate a better understanding of WCA as a new concept in hydrology. In this paper, Rc was considered the base signal ($\Delta t = 0$) and other components were considered the second signal, with Δt values varying between zero and 2π (see Fig. A). Here the period is the duration of one cycle of a wave and the frequency is the number of periods per unit of time. Both phase shift (measured in units of time) and phase angle (in radians) refer to the difference in timing of the maximal (and minimal) values in the two examined signals. The frequency is defined as the number of periods per unit of time, while the period is the duration of one wave cycle. The

temporal difference between the consecutive maximal or minimal values in the two signals is described by both phase shift (measured in units of time) and phase angle (measured in radians). The presence of phase shifts between two signals is shown by arrows; the direction of the arrows represents the positive and negative correlations between the base signal and the second signal. Here, right- and left-aligned arrows show the positive and negative correlations respectively. As shown in Fig. A, there are 8 different outcome scenarios which is possible to calculate the duration of the phase shift:

Scenario 1: Right-aligned arrows (with a Δt value of zero or 2π) represent no phase shift between two signals.

Scenario 2: Arrows inclined downwards but to the right (with $0 < \Delta t < \pi/2$) represent a phase shift of less than one fourth of a period between two signals.

Scenario 3: Upward arrows (with $\Delta t = \pi/2$) represent a phase shift equal to one fourth of a period between two signals.

Scenario 4: Arrows inclined upward but to the left (with $\pi/2 < \Delta t < \pi$) represent a phase shift of larger than one fourth of a period and less than half period between two signals.

Scenario 5: Left-aligned arrows (with a $\Delta t = \pi$) represent a phase shift equal to half a period between the base signal and the second signal.

Scenario 6: Arrows inclined downwards but to the left (with $\pi < \Delta t < 3\pi/2$) represent a phase shift of larger than one fourth of a period and less low than half of a period.

Scenario 7: Downward arrows (with a $\Delta t = 3\pi/2$) represent a phase shift equal to one fourth of a period between examined signals.

Scenario 8: Arrows inclined downwards but to the right (with $3\pi/2 < \Delta t < 2\pi$) represent a phase shift of less than one fourth of a period between the base signal and the second signal.

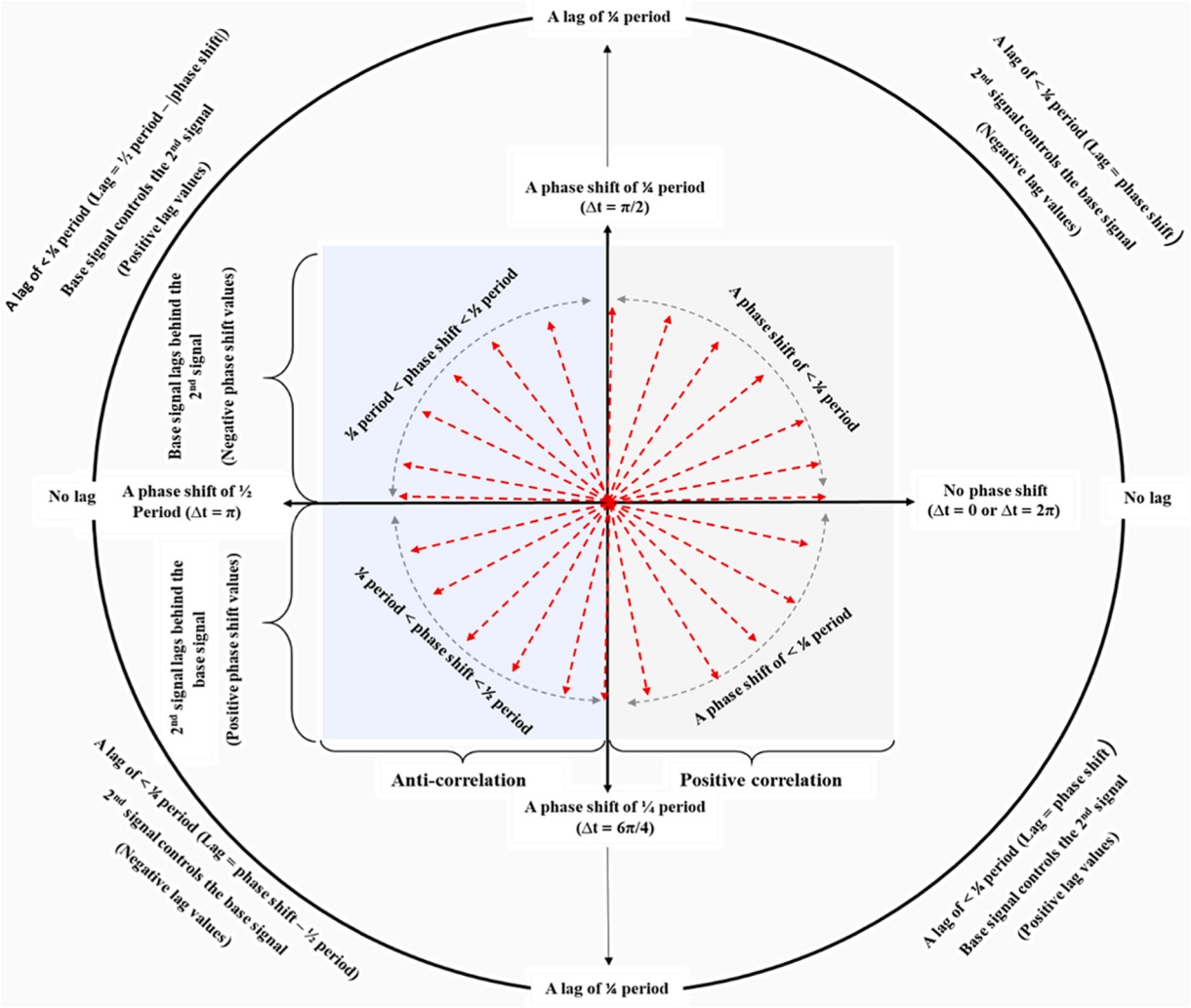

Fig. A. Phase shift, lag, correlations, and arrow directions on wavelet map between base signal and second signal.

.

References

Alpert, P., Ben-Gai, T., Baharad, A., Benjamini, Y., Yekutieli, D., Colacino, M., Diodato, L., Ramis, C., Homar, V., Romero, R., Michaelides, S., Manes, A., 2002. The paradoxical increase of Mediterranean extreme daily rainfall in spite of decrease in total values, 31-31-31-4 Geophys. Res. Lett. 29 (11). https://doi.org/10.1029/2001GL013554.

Altava-Ortiz, V., Llasat, M.C., Ferrari, E., Atencia, A., Sirangelo, B., 2011. Monthly rainfall changes in Central and Western Mediterranean basins, at the end of the 20th and beginning of the 21st centuries. Int. J. Climatol. 31, 1943–1958. https://doi.org/10.1002/joc.2204.

Arnell, N.W., 1999. Climate change and global water resources. Glob. Environ. Change 9 (SUPPL.), 31–49. https://doi.org/10.1016/S0959-3780(99)00017-5.

Asfaw, A., Simane, B., Hassen, A., Bantider, A., 2018. Variability and time series trend analysis of rainfall and temperature in northcentral Ethiopia: a case study in Woleka sub-basin. Weather Clim. Extrem. 19, 29–41. https://doi.org/10.1016/j.wace.2017.12.002.

Astuti, I.S., Sahoo, K., Milewski, A., Mishra, D.R., 2019. Impact of land use land cOver (LULC) change on surface runoff in an increasingly urbanized tropical watershed. Water Resour. Manag. 33 (12), 4087–4103. https://doi.org/10.1007/s11269-019-02320-w.

Baattrup-Pedersen, A., Garssen, A., Göthe, E., Hoffmann, C.C., Oddershede, A., Riis, T., van Bodegom, P.M., Larsen, S.E., Soons, M., 2018. Structural and functional responses of plant communities to climate change-mediated alterations in the hydrology of riparian areas in temperate Europe. Ecol. Evol. 8 (8), 3797–4366. https://doi.org/10.1002/ece3.3973.

Bauwens, A., Sohier, C., Degré, A., 2011. Hydrological response to climate change in the Lesse and the Vesdre catchments: Contribution of a physically based model (Wallonia, Belgium). Hydrol. Earth Syst. Sci. 15 (6), 1745–1756. https://doi.org/10.5194/hess-15-1745-2011.

Bedient, P.B., Huber, W.C., Vieux, B.E., 2008. Hydrology and floodplain analysis. In: Upper Saddle River, Vol. 816. Prentice Hall, NJ.

Bertola, M., Viglione, A., Vorogushyn, S., Lun, D., Merz, B., Blöschl, G., 2021. Do small and large floods have the same drivers of change? A regional attribution analysis in Europe. Hydrol. Earth Syst. Sci. 25 (3), 1347–1364. https://doi.org/10.5194/hess-25-1347-2021.

Birhanu, A., Masih, I., van der Zaag, P., Nyssen, J., Cai, X., 2019. Impacts of land use and land cover changes on hydrology of the Gumara catchment, Ethiopia. Phys. Chem. Earth, Parts A/B/C. 112, 165–174. https://doi.org/10.1016/j.pce.2019.01.006.

Bosshard, T., Kotlarski, S., Zappa, M., Schär, C., 2014. Hydrological Climate-Impact Projections for the Rhine River: GCM–RCM Uncertainty and Separate Temperature and Precipitation Effects. J. Hydrometeorol. 15 (2), 697–713. https://doi.org/10.1175/JHM-D-12-098.1.

Boulain, N., Cappelaere, B., Séguis, L., Favreau, G., Gignoux, J., 2009. Water balance and vegetation change in the Sahel: A case study at the watershed scale with an eco-hydrological model. J. Arid Environ. 73 (12), 1125–1135. https://doi.org/10.1016/j.jaridenv.2009.05.008.

Burak, S., Bilge, A.H., Ulker, D., 2021. Computation of monthly runoff coefficients for Istanbul. Therm. Sci. 25 (2 Part B), 1561–1572. https://doi.org/10.2298/TSCI191102147B.

Ceballos, A., Schnabel, S., 1998. Hydrological behaviour of a small catchment in the dehesa landuse system (Extremadura, SW Spain). J. Hydrol. 210 (1–4), 146–160. https://doi.org/10.1016/S0022-1694(98)00180-2.

Chahine, M.T., 1992. The hydrological cycle and its influence on climate. Nature 359 (6394), 373–380. https://doi.org/10.1038/359373a0.

Chen, L., Liu, C., Li, Y., Wang, G., 2007. Impacts of climatic factors on runoff coefficients in source regions of the Huanghe River. Chin. Geogr. Sci. 17 (1), 047–055. https://doi.org/10.1007/s11769-007-0047-4.

Chen, X., Parajka, J., Széles, B., Strauss, P., Blöschl, G., 2020. Controls on event runoff coefficients and recession coefficients for different runoff generation mechanisms identified by three regression methods. J. Hydrol. Hydromech. 68 (2), 155–169. https://doi.org/10.2478/johh-2020-0008.

Danáčová, M., Földes, G., Labat, M.M., Kohnová, S., Hlavčová, K., 2020. Estimating the effect of deforestation on runoin small mountainous basins in slovakia. Water (Switz.) 12 (11), 3113. https://doi.org/10.3390/w12113113.

Dari, J., Flammini, A., Morbidelli, R., Rahi, A., Saltalippi, C., 2023. Evolution of freshwater availability in a climate-changing Mediterranean context: the case of Umbria region, central Italy. Under review in Hydrological Processes.

Darvini, G., Memmola, F., 2020. Assessment of the impact of climate variability and human activities on the runoff in five catchments of the Adriatic Coast of south-central Italy. J. Hydrol.: Reg. Stud. 31, 100712 https://doi.org/10.1016/j.ejrh.2020.100712.

Descroix, L., Mahé, G., Lebel, T., Favreau, G., Galle, S., Gautier, E., Olivry, J.-C., Albergel, J., Amogu, O., Cappelaere, B., Dessouassi, R., Diedhiou, A., le Breton, E., Mamadou, I., Sighomnou, D., 2009. Spatio-temporal variability of hydrological regimes around the boundaries between Sahelian and Sudanian areas of West Africa: A synthesis. J. Hydrol. 375 (1–2), 90–102. https://doi.org/10.1016/j.jhydrol.2008.12.012.

Dey, P., Mishra, A., 2017. Separating the impacts of climate change and human activities on streamflow: A review of methodologies and critical assumptions. J. Hydrol. 548, 278–290. https://doi.org/10.1016/j.jhydrol.2017.03.014.

Dore, M.H.I., 2005. Climate change and changes in global precipitation patterns: What do we know? In Environment International. In: Elsevier Ltd, 31, pp. 1167–1181. https://doi.org/10.1016/j.envint.2005.03.004.

Fonseca, A.R., Santos, J.A., 2019. Predicting hydrologic flows under climate change: The Tâmega Basin as an analog for the Mediterranean region. Sci. Total Environ. 668, 1013–1024. https://doi.org/10.1016/j.scitotenv.2019.01.435.

Gedefaw, M., Yan, D., Wang, H., Qin, T., Wang, K., 2019. Analysis of the recent trends of two climate parameters over two eco-regions of Ethiopia. Water (Switz.) 11 (1), 161. https://doi.org/10.3390/w11010161.

Gentilucci, M., Barbieri, M., Lee, H.S., Zardi, D., 2019. Analysis of rainfall trends and extreme precipitation in the middle adriatic side, Marche Region (Central Italy). Water (Switz.) 11 (9), 1948. https://doi.org/10.3390/w11091948.

Graf, A., Bogena, H.R., Drüe, C., Hardelauf, H., Pütz, T., Heinemann, G., Vereecken, H., 2014. Spatiotemporal relations between water budget components and soil water content in a forested tributary catchment. Water Resour. Res. 50 (6), 4837–4857. https://doi.org/10.1002/2013WR014516.

Grinsted, A., Moore, J.C., Jevrejeva, S., 2004. Application of the cross wavelet transform and wavelet coherence to geophysical time series. Nonlinear Process. Geophys. 11 (5/6), 561–566. https://doi.org/10.5194/npg-11-561-2004.

Grossman, A., Morlet, J., 1984. Decomposition of hardy functions into square integrable wavelets of constant shape. SIAM J. Math. Anal. 15 (4), 723–736. https://doi.org/10.1137/0515056.

Guo, M., Ma, S., Wang, L.-J., Lin, C., 2021. Impacts of future climate change and different management scenarios on water-related ecosystem services: A case study in the Jianghuai ecological economic Zone, China. Ecol. Indic. 127, 107732 https://doi.org/10.1016/j.ecolind.2021.107732.

Ha, D.T.T., Azar, M.G., Bae, D.H., 2019. Long-term variation of runoff coefficient during dry and wet seasons due to climate change. Water 11 (11), 2411. https://doi.org/10.3390/w11112411.

Intergovernmental Panel on Climate Change IPCC, 2022. In: Climate Change 2022: Impacts, Adaptation and Vulnerability. Cambridge University Press. Cambridge, UK and New York, NY, USA, pp. 37–118 doi:10.1017/9781009325844.002. Accessed 16 July 2023.

Kendall, M.G., 1975. Rank Correlation Methods, Griffin, London.

Khanal, S., Lutz, A.F., Kraaijenbrink, P.D.A., van den Hurk, B., Yao, T., Immerzeel, W.W., 2021. Variable 21st Century Climate Change Response for Rivers in High Mountain Asia at Seasonal to Decadal Time Scales. Water Resour. Res. 57 (5) https://doi.org/10.1029/2020WR029266.

Kundzewicz, Z.W., 2008. Climate change impacts on the hydrological cycle. Ecohydrol. Hydrobiol. 8 (2–4) https://doi.org/10.2478/v10104-009-0015-y.

Labat, D., Ronchail, J., Callede, J., Guyot, J.L., de Oliveira, E., Guimarães, W., 2004. Wavelet analysis of Amazon hydrological regime variability. Geophys. Res. Lett. 31 (2) https://doi.org/10.1029/2003GL018741.

Labat, D., 2005. Recent advances in wavelet analyses: Part 1. A review of concepts. J. Hydrol. 314 (1–4), 275–288. https://doi.org/10.1016/j.jhydrol.2005.04.003.

Lauzon, N., Anctil, F., Petrinovic, J., 2004. Characterization of soil moisture conditions at temporal scales from a few days to annual. Hydrol. Process. 18 (17), 3235–3254. https://doi.org/10.1002/hyp.5656.

Li, Z., Liu, D., Li, X.Y., Wu, H., Li, G.Y., Li, Y.T., 2016. Runoff coefficient characteristics and its dominant influencing factors in a riparian grassland in the Qinghai Lake watershed, NE Qinghai-Tibet Plateau. Arab. J. Geosci. 9 (5) https://doi.org/10.1007/s12517-016-2404-z.

Li, Z., Wang, Y., Zhang, H., Chang, J., Yu, Y., 2022. Runoff response to changing environment in Loess Plateau, China: implications of the influence of climate, land use/land cover, and water withdrawal changes. J. Hydrol. 613, 128458 https://doi.org/10.1016/j.jhydrol.2022.128458.

Liu, W., Feng, Q., Deo, R.C., Yao, L., Wei, W., 2020. Experimental study on the rainfall-runoff responses of typical urban surfaces and two green infrastructures using scale-based models. Environ. Manag. 66 (4), 683–693. https://doi.org/10.1007/s00267-020-01339-9.
Longobardi, A., Villani, P., 2010. Trend analysis of annual and seasonal rainfall time series in the Mediterranean area. Int. J. Climatol. 30 (10), 1538–1546. https://doi.org/10.1002/joc.2001.
Mann, H.B., 1945. Nonparametric tests against trend. Econometrica 13 (3), 245–259. https://doi.org/10.2307/1907187.
Maragno, D., Gaglio, M., Robbi, M., Appiotti, F., Fano, E.A., Gissi, E., 2018. Fine-scale analysis of urban flooding reduction from green infrastructure: an ecosystem services approach for the management of water flows. Ecol. Model. 386, 1–10. https://doi.org/10.1016/j.ecolmodel.2018.08.002.
Marchi, L., Borga, M., Preciso, E., Gaume, E., 2010. Characterisation of selected extreme flash floods in Europe and implications for flood risk management. J. Hydrol. 394 (1–2), 118–133. https://doi.org/10.1016/j.jhydrol.2010.07.017.
Merz, R., Blöschl, G., Parajka, J., 2006. Spatio-temporal variability of event runoff coefficients. J. Hydrol. 331 (3–4), 591–604. https://doi.org/10.1016/j.jhydrol.2006.06.008.
Merz, R., Blöschl, G., 2009. A regional analysis of event runoff coefficients with respect to climate and catchment characteristics in Austria. Water Resour. Res. 45 (1) https://doi.org/10.1029/2008WR007163.
Milly, P.C.D., Dunne, K.A., Vecchia, A.V., 2005. Global pattern of trends in streamflow and water availability in a changing climate. Nature 438 (7066), 347–350. https://doi.org/10.1038/nature04312.
Morbidelli, R., Saltalippi, C., Flammini, A., Corradini, C., Wilkinson, S.M., Fowler, H.J., 2018. Influence of temporal data aggregation on trend estimation for intense rainfall. Adv. Water Resour. 122, 304–316. https://doi.org/10.1016/j.advwatres.2018.10.027.
Muñoz-Sabater, J., Dutra, E., Agustí-Panareda, A., Albergel, C., Arduini, G., Balsamo, G., Boussetta, S., Choulga, M., Harrigan, S., Hersbach, H., Martens, B., Miralles, D.G., Piles, M., Rodríguez-Fernández, N.J., Zsoter, E., Buontempo, C., Thépaut, J.-N., 2021. ERA5-Land: a state-of-the-art global reanalysis dataset for land applications. Earth Syst. Sci. Data 13, 4349–4383. https://doi.org/10.5194/essd-2021-82.
Ndhlovu, G.Z., Woyessa, Y.E., 2021. Evaluation of streamflow under climate change in the Zambezi river basin of Southern Africa. Water 13 (21), 3114. https://doi.org/10.3390/w13213114.
Norbiato, D., Borga, M., Merz, R., Blöschl, G., Carton, A., 2009. Controls on event runoff coefficients in the eastern Italian Alps. J. Hydrol. 375 (3–4), 312–325. https://doi.org/10.1016/j.jhydrol.2009.06.044.
Penna, D., Tromp-van Meerveld, H.J., Gobbi, A., Borga, M., Dalla Fontana, G., 2011. The influence of soil moisture on threshold runoff generation processes in an alpine headwater catchment. Hydrol. Earth Syst. Sci. 15 (3), 689–702. https://doi.org/10.5194/hess-15-689-2011.
Piro, P., Carbone, M., de Simone, M., Maiolo, M., Bevilacqua, P., Arcuri, N., 2018. Energy and hydraulic performance of a vegetated roof in sub-mediterranean climate. Sustainability 10 (10), 3473. https://doi.org/10.3390/su10103473.
Qiao, L., Zuo, Z., Xiao, D., Bu, L., 2021. Detection, attribution, and future response of global soil moisture in summer. Front. Earth Sci. 9 https://doi.org/10.3389/feart.2021.745185.
Rahmati, M., Groh, J., Graf, A., Pütz, T., Vanderborght, J., Vereecken, H., 2020. On the impact of increasing drought on the relationship between soil water content and evapotranspiration of a grassland. Vadose Zone J. 19 (1) https://doi.org/10.1002/vzj2.20029.
Rascón-Ramos, A.E., Martínez-Salvador, M., Sosa-Pérez, G., Villarreal-Guerrero, F., Pinedo-Alvarez, A., Santellano-Estrada, E., 2021. Hydrological behavior of a semi-dry forest in Northern Mexico: factors controlling surface runoff. Arid Land Res. Manag. 35 (1), 83–103. https://doi.org/10.1080/15324982.2020.1783026.
Rebetez, M., Mayer, H., Dupont, O., Schindler, D., Gartner, K., Kropp, J.P., Menzel, A., 2006. Heat and drought 2003 in Europe: a climate synthesis. Ann. For. Sci. 63 (6), 569–577. https://doi.org/10.1051/forest:2006043.
Regasa, M.S., Nones, M., Adeba, D., 2021. A review on land use and land cover change in ethiopian basins. Land 10 (6), 585. https://doi.org/10.3390/land10060585.
Robinet, J., Minella, J.P.G., de Barros, C.A.P., Schlesner, A., Lücke, A., Ameijeiras-Mariño, Y., Opfergelt, S., Vanderborght, J., Govers, G., 2018. Impacts of forest conversion and agriculture practices on water pathways in Southern Brazil. Hydrol. Process. 32 (15), 2304–2317. https://doi.org/10.1002/hyp.13155.
Rose, S., Peters, N.E., 2001. Effects of urbanization on streamflow in the Atlanta area (Georgia, USA): a comparative hydrological approach. Hydrol. Process. 15 (8), 1441–1457. https://doi.org/10.1002/hyp.218.
Rouse, W.R., Douglas, M.S.V., Hecky, R.E., Hershey, A.E., Kling, G.W., Lesack, L., Marsh, P., Mcdonald, M., Nicholson, B.J., Roulet, N.T., Smol, J.P., 1997. Effects of climate change on the freshwaters of arctic and subarctic North America. Hydrol. Process. 11 (8), 873–902. https://doi.org/10.1002/(SICI)1099-1085(19970630)11:8<873::AID-HYP510>3.0.CO;2-6.
Schneider, U., Finger, P., Meyer-Christoffer, A., Rustemeier, E., Ziese, M., Becker, A., 2017. Evaluating the hydrological cycle over land using the newly-corrected precipitation climatology from the Global Precipitation Climatology Centre (GPCC). Atmosphere 8 (3). https://doi.org/10.3390/atmos8030052.
Shao, Q., Li, Z., Xu, Z., 2010. Trend detection in hydrological time series by segment regression with application to Shiyang River Basin. Stoch. Environ. Res. Risk Assess. 24 (2), 221–233. https://doi.org/10.1007/s00477-009-0312-4.
Sheffield, J., Wood, E.F., 2008. Global trends and variability in soil moisture and drought characteristics, 1950-2000, from observation-driven simulations of the terrestrial hydrologic cycle. J. Clim. 21 (3), 432–458. https://doi.org/10.1175/2007JCLI1822.1.
Sherman, L.K., 1932. On runoff. In: Transactions, American Geophysical Union, 13, p. 298. https://doi.org/10.1029/TR013i001p00298-1.
Si, B.C., 2008. Spatial scaling analyses of soil physical properties: a review of spectral and wavelet methods. Vadose Zone J. 7 (2), 547–562. https://doi.org/10.2136/vzj2007.0040.
Sivakumar, B., 2011. Global climate change and its impacts on water resources planning and management: assessment and challenges. Stoch. Environ. Res. Risk Assess. 25 (4), 583–600. https://doi.org/10.1007/s00477-010-0423-y.
Sivapalan, M., Blöschl, G., Merz, R., Gutknecht, D., 2005. Linking flood frequency to long-term water balance: Incorporating effects of seasonality. Water Resour. Res. 41 (6) https://doi.org/10.1029/2004WR003439.
Song, S., Wang, W., 2019. Impacts of antecedent soil moisture on the rainfall–runoff transformation process based on high-resolution observations in soil tank experiments. Water 11 (2), 296. https://doi.org/10.3390/w11020296.
Sperna Weiland, F.C., van Beek, L.P.H., Kwadijk, J.C.J., Bierkens, M.F.P., 2012. Global patterns of change in discharge regimes for 2100. Hydrol. Earth Syst. Sci. 16 (4), 1047–1062. https://doi.org/10.5194/hess-16-1047-2012.
Sriwongsitanon, N., Taesombat, W., 2011. Effects of land cover on runoff coefficient. J. Hydrol. 410 (3–4), 226–238. https://doi.org/10.1016/j.jhydrol.2011.09.021.
Tadese, M.T., Kumar, L., Koech, R., Zemadim, B., 2019. Hydro-climatic variability: a characterisation and trend study of the Awash River Basin, Ethiopia. Hydrology 6 (2), 35. https://doi.org/10.3390/hydrology6020035.
Tan, M.L., Samat, N., Chan, N.W., Lee, A.J., Li, C., 2019. Analysis of precipitation and temperature extremes over the Muda River Basin, Malaysia. Water 11 (2), 283. https://doi.org/10.3390/w11020283.
Truong, N.C.Q., Nguyen, H.Q., Kondoh, A., 2018. Land use and land cover changes and their effect on the flow regime in the upstream Dong Nai River Basin, Vietnam. Water (Switz.) 10 (9), 1206. https://doi.org/10.3390/w10091206.
Vargas, R., Detto, M., Baldocchi, D.D., Allen, M.F., 2010. Multiscale analysis of temporal variability of soil CO 2 production as influenced by weather and vegetation. Glob. Change Biol. 16 (5), 1589–1605. https://doi.org/10.1111/j.1365-2486.2009.02111.x.
Velpuri, N.M., Senay, G.B., 2013. Analysis of long-term trends (1950–2009) in precipitation, runoff and runoff coefficient in major urban watersheds in the United States. Environ. Res. Lett. 8 (2), 024020 https://doi.org/10.1088/1748-9326/8/2/024020.
Wilk, J., Hughes, D.A., 2002. Simulating the impacts of land-use and climate change on water resource availability for a large south Indian catchment. Hydrol. Sci. J. 47, 19–30. https://doi.org/10.1080/02626660209492904.
World Meteorological Organization WMO, 2022. Temperatures in Europe increase more than twice global average. ⟨https://public.wmo.int/en/media/press-release/temperatures-europe-increase-more-twice-global-average⟩. Accessed 12 January 2023.
Xiong, J., Yin, J., Guo, S., He, S., Chen, J., Abhishek, 2022. Annual runoff coefficient variation in a changing environment: a global perspective. Environ. Res. Lett. 17 (6) https://doi.org/10.1088/1748-9326/ac62ad.

Xu, K., Milliman, J.D., Xu, H., 2010. Temporal trend of precipitation and runoff in major Chinese Rivers since 1951. Glob. Planet. Change 73 (3–4), 219–232. https://doi.org/10.1016/j.gloplacha.2010.07.002.

Yang, H., Qi, J., Xu, X., Yang, D., Lv, H., 2014. The regional variation in climate elasticity and climate contribution to runoff across China. J. Hydrol. 517, 607–616. https://doi.org/10.1016/j.jhydrol.2014.05.062.

Yue, S., Wang, C., 2004. The Mann-Kendall test modified by effective sample size to detect trend in serially correlated hydrological series. Water Resour. Manag. 18 (3), 201–218. https://doi.org/10.1023/B:WARM.0000043140.61082.60.

Zawadzki, J., Kędzior, M.A., 2014. Statistical analysis of soil moisture content changes in Central Europe using GLDAS database over three past decades. Cent. Eur. J. Geosci. 6 (3), 344–353. https://doi.org/10.2478/s13533-012-0176-x.

Zehe, E., Graeff, T., Morgner, M., Bauer, A., Bronstert, A., 2010. Plot and field scale soil moisture dynamics and subsurface wetness control on runoff generation in a headwater in the Ore Mountains. Hydrol. Earth Syst. Sci. 14 (6), 873–889. https://doi.org/10.5194/hess-14-873-2010.

Zhang, Z., Chen, X., Huang, Y., Zhang, Y., 2014. Effect of catchment properties on runoff coefficient in a karst area of southwest China. Hydrol. Process. 28 (11), 3691–3702. https://doi.org/10.1002/hyp.9920.